Technique for optimal placement of transducers for fault detection in rotating machines

Shahab Fatima, Sabyasachi G. Dastidar, Amiya Ranjan Mohanty and V.N.A Naikan

Proceedings of the Institution of Mechanical Engineers, Part O: Journal of Risk and Reliability published online 14 February 2013
DOI: 10.1177/1748006X13475412

Original Article

Institution of MECHANICAL ENGINEERS

Journal of RISK AND RELIABILITY

Proc IMechE Part O:
J Risk and Reliability
0(0) 1–13

DOI: 10.1177/1748006X13475412
pio.sagepub.com
SAGE

Technique for optimal placement of transducers for fault detection in rotating machines

Shahab Fatima[1], Sabyasachi G Dastidar[2], Amiya Ranjan Mohanty[3] and Vallayil Narayana Achutha Naikan[4]

Abstract

Online fault detection and diagnosis of rotating machinery requires a number of transducers that can be significantly expensive for industrial processes. The sensitivity of various transducers and their appropriate positioning are dependent on different types of fault conditions. It is critical to formulate a method to systematically determine the effectiveness of transducer locations for monitoring the condition of a machine. In this article, number of independent sources analysis is used as an effective tool for reducing the number of vibration sources within the system, which is then followed by principal component analysis to identify the incoherent transducers to be employed for fault detection. This experiment is conducted on a machine fault simulator for unbalanced rotor, misaligned shaft, and cracked shaft. The validation of the proposed selection process is illustrated using spectral analysis for each defect.

Keywords

Singular value decomposition, number of independent sources analysis, principal component analysis, unbalance, misalignment, cracked shaft

Date received: 27 September 2012; accepted: 2 January 2013

Introduction

Rotary machines incorporating a number of components such as shafts, bearings, rotors, electric motors, belt drives, etc., are widely used in many commercial applications and in industries. Defects occurring at each of these components, which include unbalanced rotor, misaligned shafts, cracked rotor, etc., can cause the machines to operate at lower efficiencies and unwanted effects such as excessive vibration, noise, or breakdown of the machine itself.

These problems have already been extensively explored;[1] the authors developed a model-based residual generation technique to identify misalignment and unbalance of a rotor-bearing system. In another work,[2] the transient response of a rotor system is used to distinguish a crack from coupling misalignment.

In an unknown system, it becomes crucial to identify and predict the fault before it causes severe damage. Online condition monitoring is an important tool to estimate the health of machine components by analyzing the pertinent information acquired from various sensors, which is usually unavailable without disassembling the machines. Generally, vibration signals extracted contain adequate information about the machine health status, which helps to get reliable features for the machine's condition monitoring.[3]

Characteristic features are obtained from machine parameters at the data processing stage, which can be used for fault detection by using methods such as statistical moment computation and spectral analysis.[4] However, it is time consuming and expensive to install sensors at multiple locations in an unknown system, which makes it crucial to reduce the number of permanent transducers to be installed by identifying it's most effective locations. Therefore, there is a need to

[1]Reliability Engineering Centre, Indian Institute of Technology Kharagpur, India
[2]Department of Mechanical Engineering, MNIT Jaipur, India
[3]Mechanical Engineering Department, Indian Institute of Technology Kharagpur, India
[4]Reliability Engineering Centre, Indian Institute of Technology Kharagpur, India

Corresponding author:
Amiya Ranjan Mohanty, Mechanical Engineering Department, Indian Institute of Technology Kharagpur, Kharagpur 721302, India.
Email: amohanty@mech.iitkgp.ernet.in

introduce a method that identifies the transducers that capture significant information about the machine.

A technique,[5] referred to as number of incoherent sources (NIS) analysis, has been employed for determining the number of incoherent noise-generating processes within a system. NIS analysis is accomplished by utilizing singular value decomposition (SVD), which has been used as a powerful tool in diverse fields that includes SVD-based signal processing for selection of the number of effective component signals.[6] SVD also performs well towards determining the best locations for installation of power system stabilizers,[7] and as a possible application of generalized SVD in machine condition monitoring.[8]

Principal feature analysis reduces the number of features and hence the number of sensors required.[9] Previous incoherent source identification investigation methods include the use of ordinary coherence, partial coherence,[10] and the virtual coherence function.[11]

Previously, a method was developed using principal component analysis (PCA) to determine the number of incoherent processes in a system that was subsequently combined with the virtual coherence technique to identify incoherent noise sources. PCA technique is based on the properties of SVD.[12] As one of the most extensively used multivariate statistical methods, PCA has been effectively used in dominant source identification. Moreover, utilization of PCA has also been to reduce the dimensionality of input features by devising a systematic feature selection scheme that is applied as a tool for process condition monitoring and health diagnosis.[13] In another study,[14] PCA was used to extract the low-dimensional principal component representations from the statistical features of the measured signals to monitor machine conditions.

This article applies NIS analysis and PCA to the data obtained from multiple transducers. The most effective transducers for different fault conditions in a machinery fault simulator have been identified.

Several techniques have been used for early fault detection and health monitoring of rotating machines. Dynamic stress analysis of a broken pump-turbine runner of a high-pressure machine was carried out to reveal fatigue damage.[15] A synchro and a fast rotating magnetic field (RMF)-based technique has been developed for the measurement of machine vibrations for machine condition monitoring,[16] which is further used to measure the instantaneous angular speed for low-speed machines.[17] Further advancements include shaped transducers that have been used to reduce the sensitivity of sensor output in structural health monitoring, which entails that the response can be made sensitive to particular regions of interest.[18] In addition, a monitoring system has been proposed to warn the operator of impending problems in the machining process and allows to alter and shutting down of the machining process to preserve the machine components.[19] As a result, the spectral analysis techniques can record the condition of machinery rotation even under the condition of misoperation. In the present work, the results were verified by performing spectral analysis on the vibration data acquired by the data analyzer.

In the following sections, theoretical background on NIS, SVD, and PCA is provided. This is followed by the details of the experimental study and measurements, in the results and discussion section the technique for finding out the optimum transducers for various cases of machine fault is provided, followed by a validation using spectral analysis of the measured vibration signal using the optimally selected transducers to find the actual fault in the system.

Theoretical background

NIS and SVD

The NIS analysis[5] is a stable method determining the number of incoherent processes operating in a system. The number of these processes is the number of input transducers that are required to control the system. This technique is based on the SVD of spectral density matrices of the signals measured by multiple source transducers located within the system.

SVD is an important technique for analysis of multivariate data that was first applied practically in 1958.[20] SVD has been used extensively in the past and remains a valuable tool for obtaining characterization of the structure of data.[21,22]

An [A] matrix that is composed of the auto-spectra and cross-spectra of the input transducers, for each spectral line, is decomposed into two unitary matrices and a diagonal matrix using the SVD. The equation for SVD of [A] is

$$[\mathbf{A}] = [\mathbf{U}][\mathbf{W}]\left[\mathbf{V}^{\mathbf{H}}\right] \tag{1}$$

where [U] is a unitary matrix whose columns are the eigenvectors of $[A][A^H]$, [V] is a unitary matrix whose columns are the eigenvectors of $[A^H][A]$, and [W] is a diagonal matrix whose elements are the singular values of [A]. The singular values are the square roots of the non-zero eigenvalues of $[A^H][A]$ and $[A][A^H]$. They are placed in descending order along the diagonal of the matrix [W].

Determination of NIS is accomplished by forming the [A] matrix at each spectral line. Experimental data from an array of n transducers is assembled into the [A] matrix at each frequency as

$$[\mathbf{A}] = \begin{bmatrix} S_{11} & S_{12} & \dots & S_{1n} \\ S_{21} & S_{22} & \dots & S_{2n} \\ \vdots & \vdots & \ddots & \vdots \\ S_{n1} & S_{n2} & \dots & S_{nn} \end{bmatrix} \tag{2}$$

where S_{11} is the auto-spectrum for the first reference transducer, S_{12} is the cross-spectrum between the first and the second transducer, etc. If more transducers are used than the number of actual sources, the spectral information of some channels will be linearly related to

the information of others and the [A] matrix will be rank deficient by the number of dependent channels. Thus, the rank of the [A] matrix is the number of sources sensed by the array of reference transducers.

The rank of each [A] matrix will be the number of singular values greater than the lower threshold level for the SVD of experimental data, and thus, the NIS. Once the number of input transducers is known, the best set of transducers must be identified using PCA.

PCA

PCA, introduced in 1979 is a standard technique used in the context of multivariate analysis to extract constrained information from data by reducing its dimensionality.[23] However, it retains most of the variation present in the data set. This is achieved by transforming to a new set of variables, the principle components (PCs), which are uncorrelated, and which are ordered so that the first few retain most of the variation present in all of the original variables.[24–26]

There are various ways of approaching and implementing PCA. The method used here is variance maximization, which follows the following four steps.

1. Compute the covariance of a matrix that consists of a number of data vectors, i.e. $A = [a_1,a_2,a_3,\ldots\ldots a_n]^T$ as

$$S = \frac{1}{n}\sum_{i=1}^{n} A_i * A_i^T \quad (3)$$

The variances of each vector are found on the diagonal, while the covariance of two vectors from A is found at the corresponding location in S.

2. Diagonalize the covariance matrix, S by finding its eigenvectors and eigenvalues

$$S * v = \lambda * v \quad (4)$$

where v is the eigenvector of S and is arranged in descending order, λ is the corresponding eigenvalue.

The eigenvalues are selected in decreasing order to select the vectors that contribute the most first. Therefore, the principal components of A are the eigenvectors of A's covariance matrix, S and the corresponding eigenvalue is the variance of A along the associated vector in the basis.[12]

3. Each principal component has a corresponding eigenvalue that indicates the extent to which it contributes to the final reconstruction of the data.[26] Most of the information is contained in the eigenvectors that correspond to the front few biggest eigenvalues. It is expected that the first few principal components will provide the majority of the original data, and that there will at some point be a sharp fall in the eigenvalues, indicating that the threshold has been reached.

Study on different types of faults

Vibration monitoring is one of the primary techniques for fault detection of rotating machines that generates vibration primarily owing to the presence of the following sources.

Shaft misalignment in rotating machinery can generate reaction forces and moments in the coupling, which leads to excessive vibrations causing machine faults.[2] It is a condition caused by improper assembly that results in eccentricity between the shafts of the driving and driven machines. Spectral analysis of shaft misalignment represents a series of harmonics of the shaft running speed.

Rotor unbalance is a condition in which the center of mass of a rotating disk is not coincident with the center of rotation. It exists in a rotor when vibratory force or motion is imparted to its bearings as a result of centrifugal forces. Unbalance in a rotor system is inescapable and it cannot be exterminated fully.[1]

Cracked shaft is a very common phenomenon that produces symptoms similar to coupling misalignment.[2] Unexplainable changes in the amplitude and phase of synchronous (1×) rotational speed is the most important manifestation of a shaft crack.[27–28] The asymmetry of the shaft is also indicated by the occurrence of a 2× rotational speed component.

Experiment and details

Experimental set-up

For our study, the proposed methodologies are executed on a machinery fault simulator (MFS) as shown in Figure 1(a) and mounted transducers and corresponding locations are shown in Figure 1(b). Vibrations of the drive end (DE) bearing and non-drive end (NDE) bearing were measured in three directions with B&K (Bruel & Kjaer, Denmark) 4321 tri-axial accelerometers. One accelerometer B&K 4370 was mounted on the base plate of the MFS.

Seven channels of data from the respective transducers were acquired and recorded simultaneously using Yokogawa (Yokogawa, Japan) DL850 Data Recorder at 20 KSamples/s sampling frequency and 10,000 digital samples were acquired for spectral analysis using a B&K PULSE analyzer.

Measurements

Experiment was designed to study the effectiveness of transducer for multiple faults on the MFS. All seven channels of signal data were measured for the rotational speed of 600, 900, 1200, 1500, and 1800 r/min. Results are analyzed for all the rotational speeds since

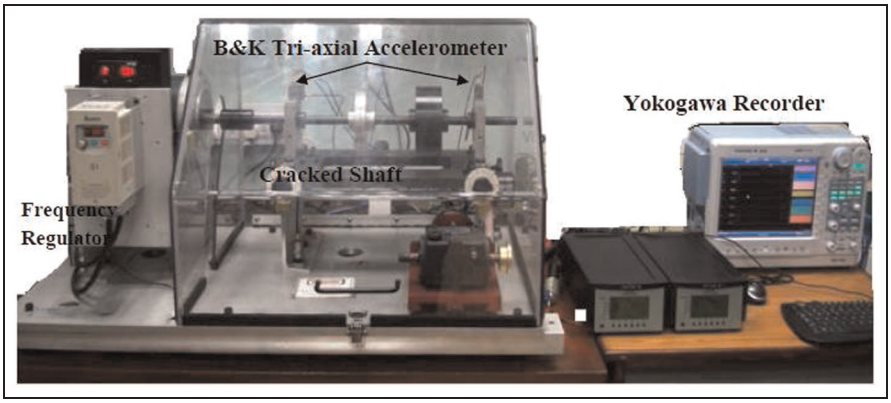

Figure 1(a). Machinery fault simulator set-up.

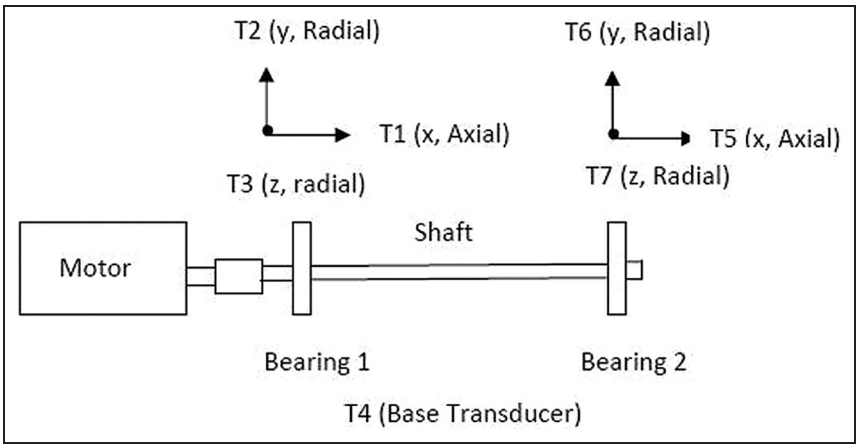

Figure 1(b). Schematic representation of mounted transducers and corresponding locations.

Table 1(a). Specifications of the MFS used for experiment.

Induction motor electrical frequency	50 Hz
Distance between drive end and non-drive end bearings	36.2 cm
Distance between drive end and non-drive bolts of motor	7.62 cm
Shaft diameter	1.58 cm
Shaft loader	5 kg

Table 1(b). Different conditions of faults in MFS.

Sl. No.	Different conditions in machinery fault simulator
1	Aligned (normal)
2	Misalignment
3	Unbalance
4	Unbalance and misalignment
5	Cracked shaft (bolt fully tightened)
6	Cracked shaft (bolt partially tightened)
7	Normal shaft with shaft loader
8	Normal shaft with shaft loader and unbalance

the conclusions are the same. So, results are reported only for 1200 and 1800 r/min. Specifications of the MFS used for the experiments are given in Table 1(a).

The seven channel signal data were obtained for the perfect (aligned) shaft condition of MFS followed at seven fault conditions as shown in Table 1(b).

Angular misalignment was introduced using shims (thickness 0.062 cm) on the NDE bearing side of the base plate. Unbalance was created by fixing masses onto the rotor disk (each mass weighs 6.13 g). For performing the experiment on the crack shaft, the perfect shaft was replaced by a flange-simulated cracked shaft. Figure 2 shows the flanged simulated cracked shaft, which consists of two separable shafts joined at the mating flanges, and Figure 3 shows the view of the cracked shaft joined by the four bolts and disjoined conditions.

For inducing crack in a shaft, four bolts are loosened or tightened. A large black disk next to flanges provides load on the shaft owing to its heavy weight. For experimental simulation, two bolts were loosened for introducing crack and this condition is known as 'bolts partially tightened', which was more serious than 'bolts fully tightened' where four bolts were tightened.

Results and discussion

Determination of the NIS

Using the spectral information obtained from the data analyzer, the [A] matrix was formed at each frequency

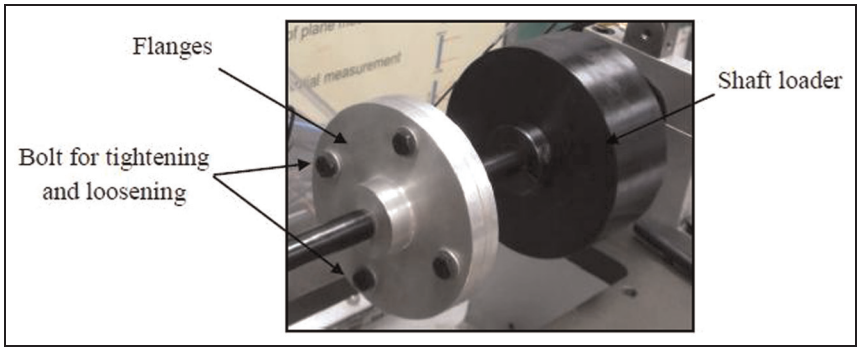

Figure 2. Cracked shaft with the two flanges for varying the amount of crack.

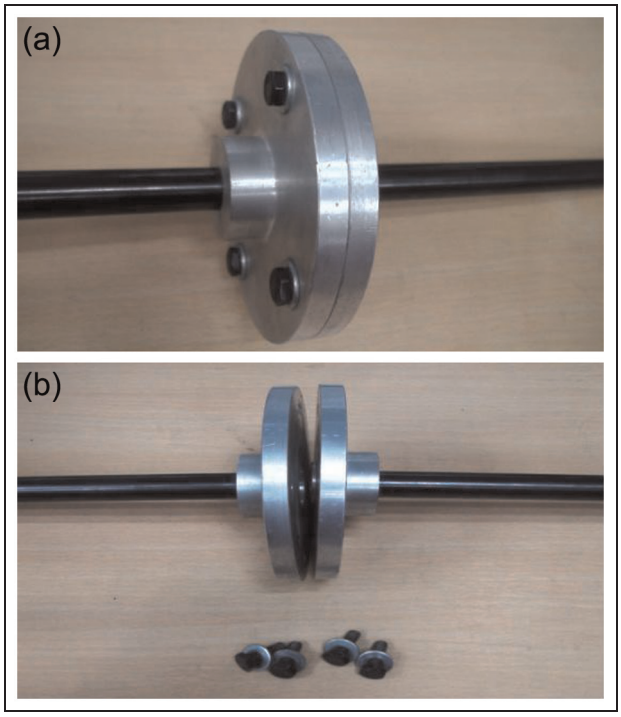

Figure 3. View of the cracked shaft: (a) joined by the four bolts; (b) disjointed.

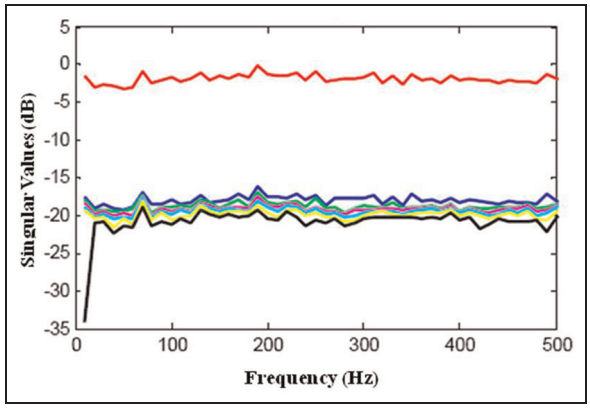

Figure 4. Singular values of the seven transducer signals mounted on MFS at normal condition.

for the seven transducers. The NIS analysis was performed on the [A] matrix. The singular values from the [A] matrix are shown in Figure 4. The values are plotted on a semi-logarithmic scale over the 0–500 Hz frequency range.

The threshold value is estimated as the value below which the singular values remain constant with frequency. In Figure 4, the second singular value remains near –18 dB over the entire frequency range. Thus, an insignificant amount of information is contained from the remaining six transducer. The singular values that are larger than the threshold value are the number of independent sources. In this case, one singular value is significantly greater above –18 dB. Thus, only one transducer senses the majority of the vibration in the MFS, which is the minimum number of input transducers required for effective data collection. The main purpose of NIS analysis is determining the total independent sources present in the system (in this case: one). Now, one independent source can be present at any location within the system. This is where PCA is utilized, which identifies the incoherent source(s) and its location within the system

Incoherent source identification using PCA

The data were obtained from the seven transducers for normal (aligned), misaligned, unbalanced, unbalanced–misaligned, cracked shaft with bolt partially tightened, and cracked shaft with bolt fully tightened conditions of the MFS. PCA was performed on the data followed by eigenvalue analysis of the resultant correlation matrix. The recorded vibration data is obtained at the motor speed of 1200 and 1800 r/min. Similar results were incurred from analysis of data at 1800 r/min.

PCA in normal (aligned) condition. PCA is performed on the recorded vibration data for an aligned system and the eigenvalue analysis is executed on the correlation matrix which renders the following results. Here proportion can be calculated by

Table 2(a). Eigenvalue analysis of the vibration data from the seven transducers from the normal system at 1200 r/min.

Eigenvalue	1.40	1.20	1.1	1.02	0.82	0.77	0.63
Proportion	0.20	0.17	0.16	0.15	0.11	0.11	0.09
Cumulative	0.20	0.37	0.53	0.68	0.8	0.91	1.00

Table 2(b). Correlation matrix of vibration data with PCs from a normal system at 1200 r/min.

Transducers	PC1	PC2	PC3	PC4
T1 (Axial, DE Brg.)	–0.4	–0.505	–0.163	0.253
T2 (Radial, DE Brg.)	0.102	–0.207	–0.426	–0.703
T3 (Radial, DE Brg.)	–0.137	–0.172	0.694	0.096
T4 (Vertical, Base)	0.037	–0.133	0.552	–0.613
T5 (Axial, NDE Brg.)	–0.364	–0.614	–0.07	–0.064
T6 (Radial, NDE Brg.)	–0.614	0.302	–0.006	–0.134
T7 (Radial, NDE Brg.)	–0.548	0.433	–0.043	–0.189

DE: drive end; NDE: non-drive end.

$$\text{Proportion} = \frac{\text{Eigenvalue for the component of interest}}{\text{Total eigenvalues of the correlation matrix}} \quad (5)$$

In PCA, the total eigenvalues of the correlation matrix is equal to the total number of variables being analyzed. Cumulative percent indicates the percent of variance accounted for by the present component, as well as all preceding components. They usually retain enough components so that the cumulative percent of variance accounted for is equal to some minimal value.

The last few principal components usually account for the least proportion of total variance. Therefore, only the eigenvalues of PCs greater than one are retained. In this case, the first four are retained, which explains 68% of the total variance accounted for as shown by the cumulative proportion of each principle component in Table 2(a). It is also important that the redundant components, i.e. PCs containing variables that appear in a previous PC as a significant contribution are removed.

Table 2(b) gives the weights of each original variable in the PCs for the first four components that are retained. Using this table each PC can be interpreted. Variables that have very low magnitude in a specific column have minimal contribution to that particular PC. Thus, the most significant variables in each component, i.e. those represented by high loadings, have been taken into consideration for retaining the component.

After evaluating the correlation matrix, it is obtained that in the first PC the most significant variables are sixth and seventh. Thus, the first principal component is a measure of the sixth and seventh transducer, and to some extent, first transducer, and so on. The sixth and seventh transducers show a remarkable decrease as it is negatively related to its component. The second transducer (radial transducer) shows the highest correlation as it is positively related to the PC with the highest value. Similarly, the second principal component marks a decrease in fifth and first transducer. The third principal component is a measure of the severity in correlation of transducer three and four. The fourth PC is redundant as its fourth variable, which is significant, is also a major contributor to the previous component.

The principal component that covers the most variance is that which is the most important since it contains maximum information about the data.[22] From analysis of PCs from one to four, it is concluded that the first principal component, which shows the highest eigenvalue proportion, depicts that the most prominent correlation is observed in the second transducer. Thus, that the second transducer (radial transducer) at bearing location 1 (DE) is the most effective. Also, the analysis shows that the fourth transducer (base transducer) is the most suitable to be used alongside the second transducer. The main purpose of providing two sensors in the results is to show that the second sensor is able to extract more information than the remaining five transducers. The results clearly indicate that the only one transducer is most effective. To validate the efficiency of PCA, white Gaussian noise (taking signal-to-noise ratio per sample as 10 dB) is added to the signal data and the eigenvalue analysis of the resultant signal was performed. The observations also suggest that the second transducer showed highest correlation confirming the analysis with the signal described earlier.

PCA in angular misalignment condition. From Table 3(a) and (b) it is concurred that the first principal component, which shows the highest Eigenvalue proportion, depicts the first transducer (axial) to be the most effective for misaligned condition. Also, the third transducer (radial transducer) is the most suitable to be used alongside the first transducer

PCA in unbalance condition. Observing the first principal component in Table 4(a) and (b), the sixth transducer, i.e. radial transducer, is concluded as the most effective transducer for the unbalanced rotor.

Table 3(a). Eigenvalue analysis of the vibration data from the seven transducers from a misaligned system at 1200 r/min.

Eigenvalue	1.3	1.14	1.09	1.02	0.85	0.83	0.72
Proportion	0.19	0.16	0.15	0.15	0.12	0.12	0.10
Cumulative	0.19	0.35	0.51	0.65	0.77	0.89	1.00

Table 3(b). Correlation matrix of vibration data with PCs from a misaligned system at 1200 r/min.

Transducers	PC1	PC2	PC3	PC4
T1 (Axial, DE Brg.)	–0.055	0.119	0.518	0.711
T2 (Radial, DE Brg.)	–0.158	–0.74	0.127	0.028
T3 (Radial, DE Brg.)	–0.056	0.532	0.383	–0.451
T4 (Vertical, Base)	–0.126	0.163	–0.737	0.162
T5 (Axial, NDE Brg.)	–0.503	–0.211	0.141	–0.459
T6 (Radial, NDE Brg.)	–0.588	0.29	–0.074	0.188
T7 (Radial, NDE Brg.)	–0.595	–0.008	–0.009	0.137

DE: drive end; NDE: non-drive end.

Table 4(a). Eigenvalue analysis of the vibration data from the seven transducers from an unbalanced system at 1200 r/min.

Eigenvalue	1.33	1.21	1.18	1.01	0.83	0.81	0.61
Proportion	0.19	0.17	0.16	0.14	0.12	0.12	0.08
Cumulative	0.19	0.36	0.53	0.67	0.80	0.91	1.00

Table 4(b). Correlation matrix of vibration data with PCs from an unbalanced system at 1200 r/min.

Transducers	PC1	PC2	PC3	PC4
T1 (Axial, DE Brg.)	0.005	0.679	0.036	0.117
T2 (Radial, DE Brg.)	0.071	–0.02	–0.504	–0.661
T3 (Radial, DE Brg.)	–0.012	0.025	0.697	0.02
T4 (Vertical, Base)	–0.002	–0.241	0.486	–0.645
T5 (Axial, NDE Brg.)	0.143	0.65	0.061	–0.313
T6 (Radial, NDE Brg.)	0.715	0.082	0.118	–0.046
T7 (Radial, NDE Brg.)	0.681	–0.225	–0.071	0.18

DE: drive end; NDE: non-drive end.

PCA in unbalance and misalignment condition. After performing the eigenvalue analysis on the data obtained from an unbalanced and misaligned system, the first three PCs, which have eigenvalues greater than one, are retained. As ascertained in the first PC, in Table 5(a) and (b), the second transducer, i.e. radial transducer, is the most effective transducer for combined misaligned and unbalanced defects. Also, the first (axial transducer) is the most suitable to be used alongside the second transducer.

PCA in cracked shaft (bolt partially tightened) condition. As depicted in Table 6(a) and (b), the first principal component is a measure of the increase in first and decrease in seventh transducer, which shows that the first transducer, i.e. axial transducer, is the most effective transducer for cracked shaft.

PCA in cracked shaft (bolt fully tightened) condition. After performing the eigenvalue analysis on the data obtained from a cracked shaft (bolt fully tight) system, the first three principal components that have eigenvalues greater than one were retained. As observed in the first principal component in Table 7(a) and (b), the fifth transducer, i.e. axial transducer, is the most effective transducer for cracked shaft.

PCA in normal shaft with shaft loader condition. From Table 8(a) and (b), it can be observed that the T1 (Axial, DE Brg.) transducer is the most effective transducer for PCA in normal shaft with loader condition. In this analysis, the axial transducer is more effective than the radial transducer because of the heavy load of loader.

Table 5(a). Eigenvalue analysis of the vibration data from the seven transducers from an unbalanced and misaligned system at 1200 r/min.

Eigenvalue	1.27	1.17	1.08	0.94	0.92	0.81	0.79
Proportion	0.183	0.16	0.15	0.14	0.13	0.12	0.11
Cumulative	0.18	0.35	0.50	0.64	0.77	0.88	1.00

Table 5(b). Correlation matrix of vibration data with PCs from an unbalanced and misaligned system at 1200 r/min.

Transducers	PC1	PC2	PC3	PC4
T1 (Axial, DE Brg.)	–0.258	–0.571	–0.115	–0.135
T2 (Radial, DE Brg.)	0.056	0.244	–0.692	–0.52
T3 (Radial, DE Brg.)	–0.276	–0.299	0.473	–0.583
T4 (Vertical, Base)	–0.313	–0.35	–0.39	0.526
T5 (Axial, NDE Brg.)	–0.621	–0.024	–0.244	–0.154
T6 (Radial, NDE Brg.)	–0.456	0.321	0.267	0.261
T7 (Radial, NDE Brg.)	–0.404	0.547	0.031	–0.05

DE: drive end; NDE: non-drive end.

Table 6(a). Eigenvalue analysis of the vibration data from the seven transducers from a cracked shaft (bolt partially tight) at 1200 r/min.

Eigenvalue	1.28	1.14	1.09	1.01	0.92	0.86	0.68
Proportion	0.18	0.16	0.15	0.14	0.13	0.12	0.09
Cumulative	0.18	0.35	0.504	0.64	0.77	0.90	1.00

Table 6(b). Correlation matrix of vibration data with PCs from a cracked shaft (bolt partially tight) at 1200 r/min.

Transducers	PC1	PC2	PC3	PC4
T1 (Axial, DE Brg.)	0.663	–0.034	0.137	–0.268
T2 (Radial, DE Brg.)	–0.199	–0.439	0.412	–0.182
T3 (Radial, DE Brg.)	0.192	0.336	–0.195	0.716
T4 (Vertical, Base)	0.153	0.299	–0.55	–0.576
T5 (Axial, NDE Brg.)	0.35	–0.419	–0.335	0.083
T6 (Radial, NDE Brg.)	0.209	–0.627	–0.279	0.207
T7 (Radial, NDE Brg.)	–0.543	–0.188	–0.531	–0.037

DE: drive end; NDE: non-drive end.

Table 7(a). Eigenvalue analysis of the vibration data from the seven transducers from a cracked shaft (bolt fully tight) at 1200 r/min.

Eigenvalue	1.36	1.25	1.03	0.95	0.91	0.79	0.68
Proportion	0.19	0.18	0.14	0.13	0.13	0.11	0.09
Cumulative	0.19	0.37	0.52	0.65	0.78	0.903	1.00

Table 7(b). Correlation matrix of vibration data with PCs from a cracked shaft (bolt fully tight) at 1200 r/min.

Transducers	PC1	PC2	PC3	PC4
T1 (Axial, DE Brg.)	0.425	–0.387	–0.362	0.133
T2 (Radial, DE Brg.)	0.169	0.505	–0.242	–0.519
T3 (Radial, DE Brg.)	0.258	–0.265	0.747	0.032
T4 (Vertical, Base)	–0.369	–0.511	–0.358	0.175
T5 (Axial, NDE Brg.)	0.442	0.07	–0.346	0.228
T6 (Radial, NDE Brg.)	0.18	0.442	0.06	0.753
T7 (Radial, NDE Brg.)	–0.6	0.253	–0.02	0.249

DE: drive end; NDE: non-drive end.

Table 8(a). Eigenvalue analysis of the vibration data from the seven transducers from a normal shaft with loader at 1200 r/min.

Eigenvalue	1.21	1.10	1.05	1.00	0.97	0.85	0.79
Proportion	0.17	0.15	0.15	0.14	0.13	0.12	0.11
Cumulative	0.17	0.33	0.48	0.62	0.76	0.88	1.00

Table 8(b). Correlation matrix of vibration data with PCs from a normal shaft with loader at 1200 r/min.

Transducers	PC1	PC2	PC3	PC4
T1 (Axial, DE Brg.)	–0.651	0.168	–0.098	0.063
T2 (Radial, DE Brg.)	–0.185	0.134	0.625	0.627
T3 (Radial, DE Brg.)	–0.491	0.424	0.004	–0.426
T4 (Vertical, Base)	0.211	0.722	–0.111	–0.125
T5 (Axial, NDE Brg.)	–0.135	–0.015	0.468	–0.426
T6 (Radial, NDE Brg.)	–0.120	0.350	–0.455	0.473
T7 (Radial, NDE Brg.)	0.534	–0.360	–0.401	–0.011

DE: drive end; NDE: non-drive end.

Table 9(a). Eigenvalue analysis of the vibration data from the seven transducers from a normal shaft with loader and unbalance at 1200 r/min.

Eigenvalue	1.22	1.10	1.07	1.01	0.93	0.89	0.74
Proportion	0.17	0.15	0.15	0.14	0.13	0.12	0.10
Cumulative	0.19	0.37	0.52	0.65	0.78	0.903	1.00

Table 9(b). Correlation matrix of vibration data with PCs from a normal shaft with loader and unbalance at 1200 r/min.

Transducers	PC1	PC2	PC3	PC4
T1 (Axial, DE Brg.)	0.624	0.182	–0.256	0.154
T2 (Radial, DE Brg.)	–0.145	–0.069	–0.763	–0.094
T3 (Radial, DE Brg.)	0.224	0.390	–0.361	0.450
T4 (Vertical, Base)	–0.219	0.668	–0.064	–0.005
T5 (Axial, NDE Brg.)	–0.474	–0.309	–0.403	0.175
T6 (Radial, NDE Brg.)	0.011	0.308	–0.219	–0.826
T7 (Radial, NDE Brg.)	0.516	–0.416	–0.086	–0.228

DE: drive end; NDE: non-drive end.

Table 10. Summary of effective transducers for all fault conditions simulated in MFS.

Condition of faults MFS	Effective transducer obtained
Normal (aligned)	T2 (Radial, DE Brg.)
Misalignment	T1 (Axial, DE Brg.)
Unbalance	T6 (Radial, NDE Brg.)
Unbalance and misalignment	T2 (Radial, DE Brg.)
Cracked shaft (bolt loose)	T1 (Axial, DE Brg.)
Cracked shaft (bolt tight)	T5 (Axial, NDE Brg.)
Normal shaft with shaft loader	T1 (Axial, DE Brg.)
Normal shaft with shaft loader and unbalance	T1 (Axial, DE Brg.)

DE: drive end; MFS: machinery fault simulator; NDE: non-drive end.

PCA in normal shaft with shaft loader and unbalance conditions. For this analysis also, from Table 9(a) and (b), the T1 (Axial, DE Brg.) is the most effective transducer compared with others. The effect of the unbalance does not create any difference in the system owing to the heavy load of the loader.

Experimental validation by vibration measurements

Measured vibration spectra for normal (aligned) condition. Spectral analysis was performed on data obtained from the effective transducers for each MFS-simulated fault condition (as shown in Table 10) to validate that they demonstrate the fault conditions efficiently.

The 3× components are observed (which is because of the residual unbalance) in Figure 5(a) and (b), however, the amplitude of vibration is very low, which

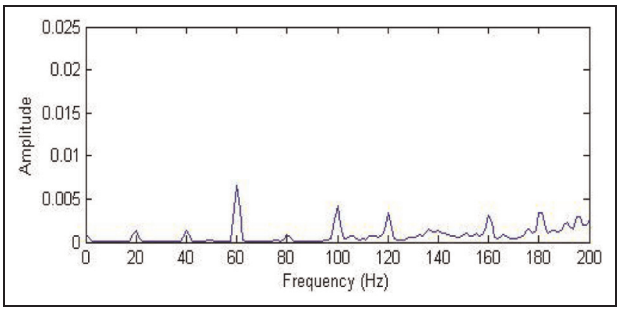

Figure 5(a). Normal condition of MFS for T2 (radial) at 1200 r/min.

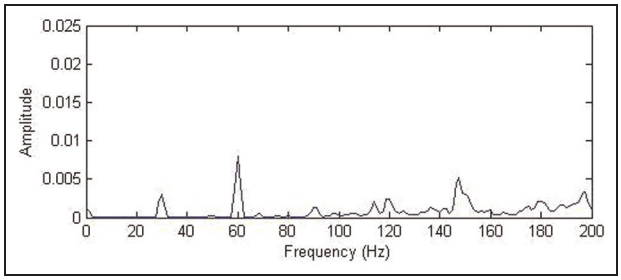

Figure 5(b). Normal condition of MFS for T2 (radial) at 1800 r/min.

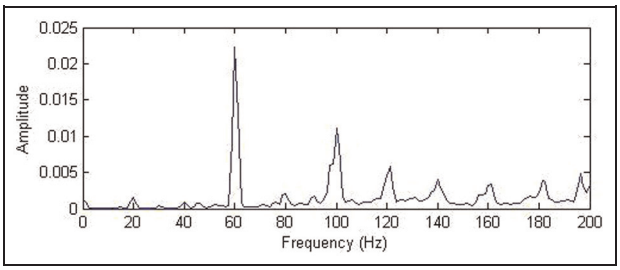

Figure 6(a). Misaligned condition of MFS for T1 (axial) at 1200 r/min.

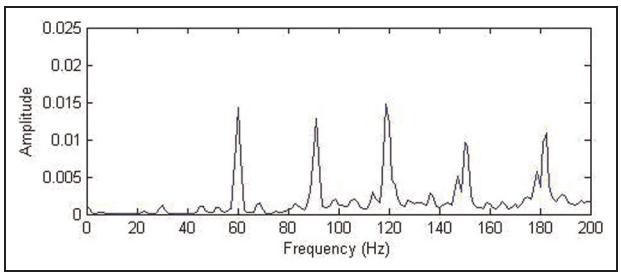

Figure 6(b). Misaligned condition of MFS for T1 (axial) at1800 r/min.

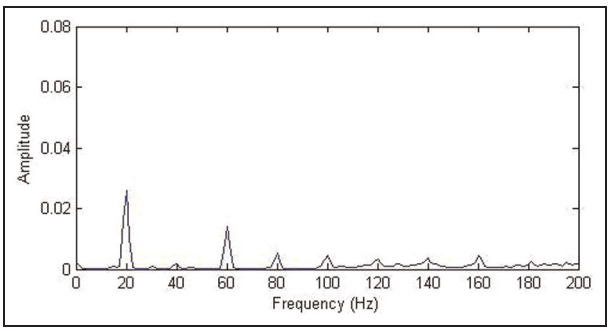

Figure 7(a). Unbalanced condition of MFS for T6 (radial) at 1200 r/min.

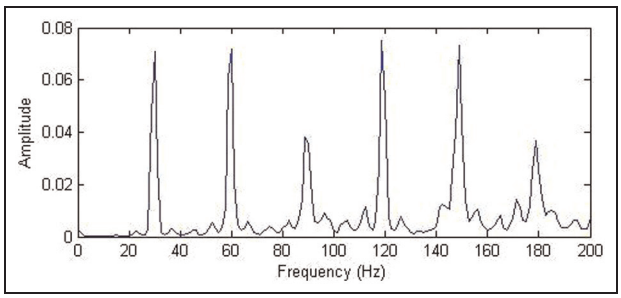

Figure 7(b). Unbalanced condition of MFS for T6 (radial) at 1800 r/min.

verifies that the T2 transducer exhibits that the MFS has no significant fault.

Measured vibration spectra for angular misalignment condition. Investigating axial forces as shown in Figure 6(a) and (b) for the T1 transducer, it is found that after introducing angular misalignment, 3× and 5× harmonics are excited and the 1× is unaffected.

This irregular pattern might be owing to the existence of axial vibrations for angular misalignment in the rotor, which confirms our selection of T1 as the effective transducer. The verification is further strengthened by the appearance of slightly excited sidebands around 3× and 5× harmonics, which depicts the presence of misalignment.

Measured vibration spectra for unbalance condition. The vibration spectrum for radial vibrations (from T6 transducer) shows a predominant 1× peak for motor speeds of 1200 r/min and 1800 r/min as shown in Figure 7(a) and (b), respectively. The presence of harmonics at 3× and 5× further affirms the fault in the rotor, i.e. rotor imbalance, which generates lateral force and vibrations. Thus, the selected T6 transducer shows the disturbances more clearly than the other transducers. It is also seen that the amplitude varies proportionately to the square of the speed.

Measured vibration spectra for unbalance and misalignment condition. No definite characteristic is observed by the spectral analysis performed on unbalanced and misaligned condition in MFS as shown in Figure 8(a) and 8(b).

However, high 1× peaks in frequency domain of both 20 Hz and 30 Hz depicts that a fault is present, which confirms the selection of T2 transducer as it demonstrates the fault evidently. The excitation of

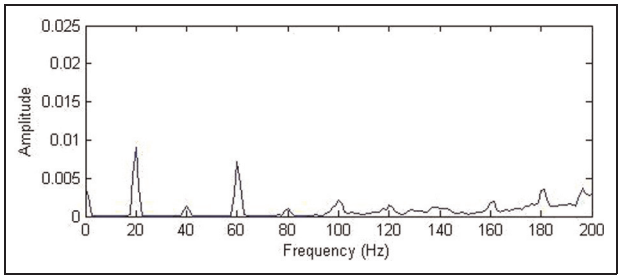

Figure 8(a). Unbalanced–misaligned condition of MFS for T2 (axial) at 1200 r/min.

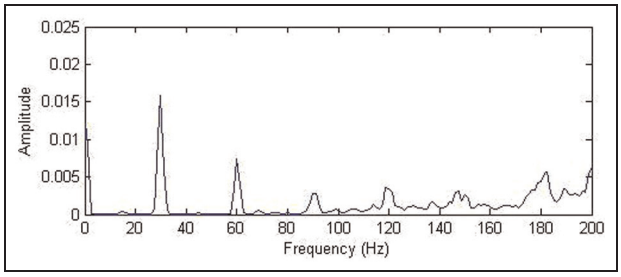

Figure 8(b). Unbalanced–misaligned condition of MFS for T2 (axial) at 1800 r/min.

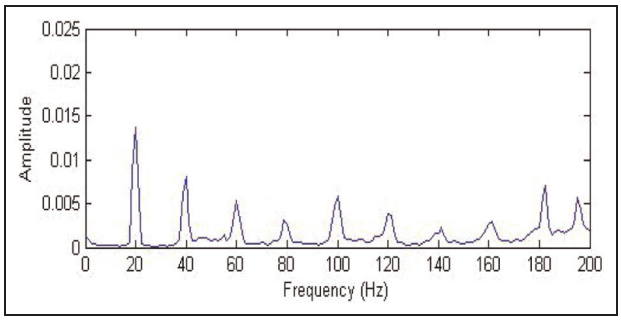

Figure 9(a). Cracked shaft (with bolt partially tightened) for T1(axial transducer) at 1200 r/min.

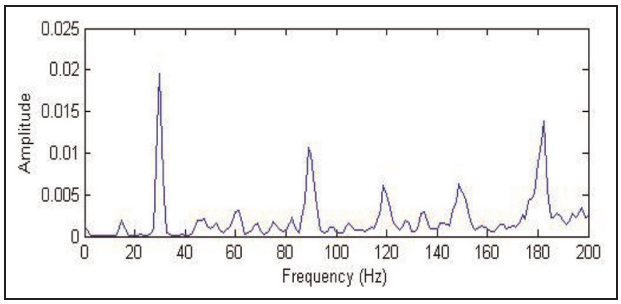

Figure 9(b). Cracked shaft (with bolt partially tightened) for T1(axial transducer) at 1800 r/min.

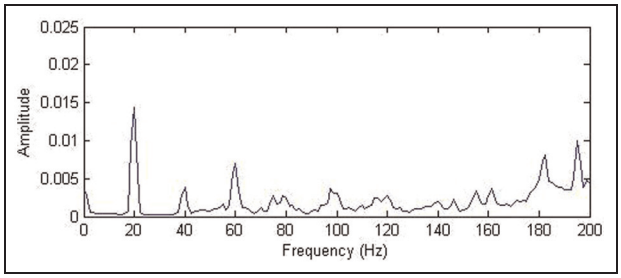

Figure 10(a). Flange simulated-cracked shaft (bolt fully tightened) for T5(axial) at 1200 r/min.

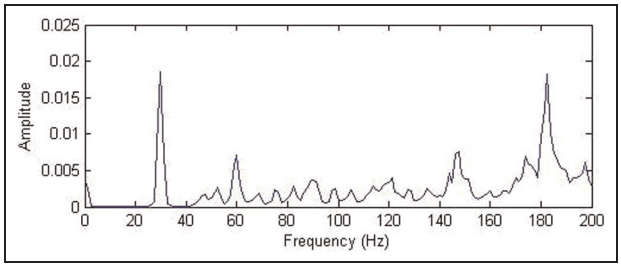

Figure 10(b). Flange simulated-cracked shaft (bolt fully tightened) for T5(axial) at 1800 r/min.

2×, 3×, 4× vibration harmonics for both the frequencies further exemplifies the presence of a fault.

Measured vibration spectra for cracked shaft (bolt partially tightened). Figure 9(a) and (b) show that the 1× and 2× frequency response for cracked shaft increased compared with the perfect shaft. The occurrence of a 2× vibration are consistent for both speeds.

This confirms the cracked shaft characteristics that show misalignment properties with high axial vibration as depicted very strongly in the T1 transducer.

Measured vibration spectra for cracked shaft (bolt fully tightened). Cracked shaft (bolt fully tightened) simulates the condition of a normal (aligned) shaft, but the vibration spectra shows different peaks owing to the use of a loader in a cracked shaft, which provides load on the shaft owing to its weight. The spectral analyses of data obtained from T5 (axial) transducer depict peaks that cannot easily be deciphered. In Figure 10(a) and (b), the 2× peaks are not well-defined. This confirms the effectiveness of T5 transducer as it successfully exhibits the features of flange simulated-cracked shaft whose bolt is fully tightened.

Measured vibration spectra for normal shaft with shaft loader. Here the axial transducer T1 is more effective than the other transducers because of the heavy load of the loader. Figure 11(a) and (b) shows the presence of harmonics at 3× and 5× further affirms the fault in the rotor, i.e. rotor imbalance, which generates lateral force and vibrations.

Measured vibration spectra for normal shaft with shaft loader and unbalance. The observations from the measured

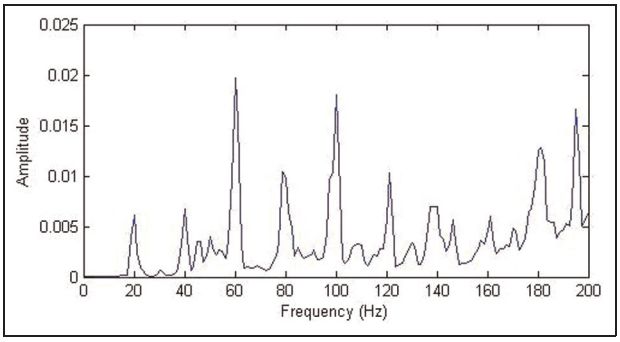

Figure 11(a). Normal shaft with loader for T1(axial) at 1200 r/min.

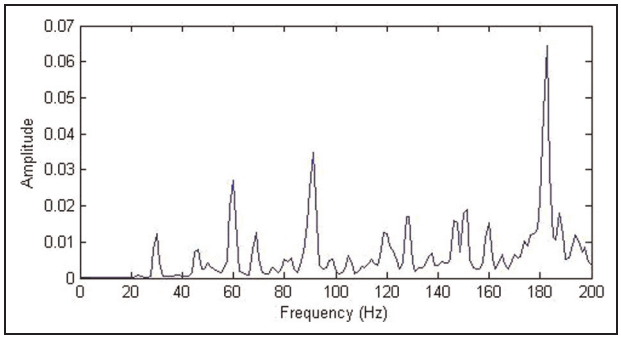

Figure 11(b). Normal shaft with loader for T1(axial) at 1800 r/min.

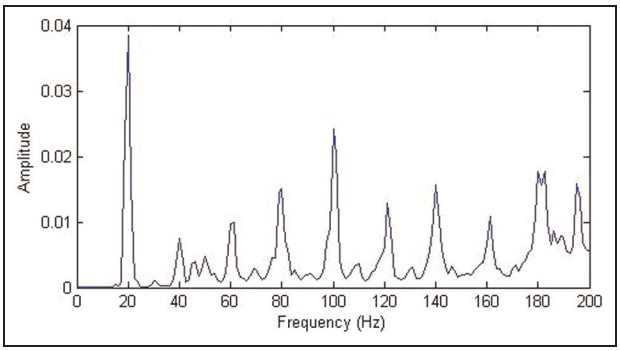

Figure 12(a). Normal shaft with loader and unbalance for T1(axial) at 1200 r/min.

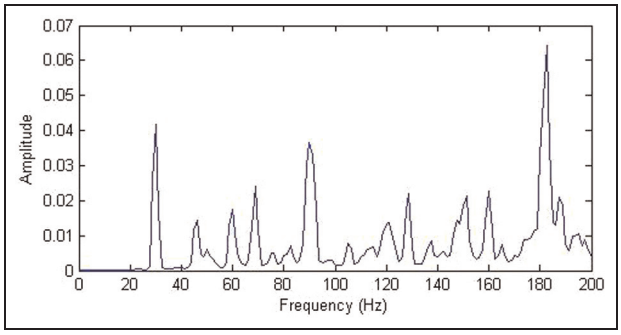

Figure 12(b). Normal shaft with loader and unbalance for T1(axial) at 1800 r/min.

vibration spectra for normal shaft with loader and unbalance condition at 1200 and 1800 r/min show the previously observed phenomenon, which is the axial transducers T1, is the most effective one. This implies that there is no effect of unbalance mass on measured spectra for this case. Figure 12(a) and (b) shows the presence of harmonics at 3× and 5× which further confirms the fault in the rotor.

Comparison with spectral analysis

An experiment on a normal shaft with a shaft loader and unbalance mass rotating at 1185 r/min on the MFS was done to validate the proposed method with traditional spectral analysis. The vibration peaks amplitude at 19.75 Hz for all the seven transducers are shown in the Table 11. It is noticed that the maximum amplitude is for transducer 1 (axial, DE), which is the same as determined by our proposed method. Thus the proposed method has been able to identify the transducer that needs to be used to monitor the condition of the machine.

Table 11. Spectral analysis comparison for normal shaft with loader and unbalance condition.

Transducers	Vibration peak amplitude at 19.75 Hz (m/s^2)
T1 (Axial, DE Brg.)	0.35
T2 (Radial, DE Brg.)	0.13
T3 (Radial, DE Brg.)	0.18
T4 (Vertical, Base)	0.12
T5 (Axial, NDE Brg.)	0.30
T6 (Radial, NDE Brg.)	0.24
T7 (Radial, NDE Brg.)	0.33

DE: drive end; NDE: non-drive end.

Conclusions

For online health monitoring of machinery, a systematic approach for selection of the most sensitive transducer locations has been carried out in this article. Owing to restrained data handling capacity, SVD has emerged as an important data reduction technique. This technique is applied in NIS analysis, which significantly reduces the number of transducers, for data collection and analysis, from seven to one. This is then merged with PCA to identify the transducer locations. This hypothesis has been tested on vibration data acquired from unbalance, misalignment, and cracked rotor conditions on a MFS. The performance of this approach was validated by conducting spectral analysis on the acquired data for each fault condition. The vibration spectrum of the selected transducer interprets the severity of the fault from the signal features more clearly than the remaining transducers. The proposed

methodology can be applied to any unknown system by a condition monitoring engineer for minimizing the number of transducers and identify the locations to mount them.

Funding

This research was made possible by funds received from the Ministry of Human Resources Development, Government of India

References

1. Jalan AK and Mohanty AR. Model based fault diagnosis of a rotor–bearings system for misalignment and unbalance under steady-state condition. *J Sound Vib* 2009; 327: 604–622.
2. Prabhakar S, Sekhar AS and Mohanty AR. Crack versus coupling misalignment in a transient Rotor system. *J Sound Vib* 2002; 256(4): 773–786.
3. He Q, Kong F and Yan R. Subspace-based gearbox condition monitoring by kernel principal component analysis. *Mech Sys Signal Process* 2007; 21: 1755–1772.
4. Zhou W, Habetler TG and Harley RG. Bearing condition monitoring for electrical machines: a general review. In: *Proceedings of international symposium on diagnosis of electric machines*, Poland, 2007, 6–8 September, pp. 3–6, IEEE Publication.
5. Kompella MS, Davies P, Bernhard RJ, et al. A technique to determine the number of incoherent sources contributing to the response of a system. *Mech Sys Signal Process* 1994; 8(4): 363–380.
6. Zhao X and Ye B. Selection of effective singular values using difference spectrum and its application to fault diagnosis of headstock. *Mech Sys Signal Process* 2011; 25: 1617–1631.
7. Karimpour A, Asgharian R and Malik OP. Determination of PSS location based on singular value decomposition. *Elec Power Energy Sys* 2005; 27: 535–541.
8. Cempel C. Generalized singular value decomposition in multidimensional condition monitoring of machines—A proposal of comparative diagnostics. *Mech Sys Signal Process* 2009; 23: 701–711.
9. Zhou J, Pang CK, Lewis FL, et al. Dominant feature identification for industrial fault detection and isolation applications. *Expert Sys Applic* 2011; 38: 10696–10684.
10. Alfredson RJ. The partial coherence for source identification on a Diesel Engine. *J Sound Vib* 1977; 55(4): 487–494.
11. Price SM and Bernhard RJ. Virtual coherence: A digital signal processing technique for incoherent source identification. In: *Proceedings of the 4th international modal analysis conference*, Los Angeles, 1986, February 3–6, pp. 1256–1262.
12. Albright MF. Conditioned source analysis, A technique for multiple input system identification with application to combustion energy separation in piston engines, 1995, SAE paper No: 951376.
13. Malhi A. PCA-Based feature selection scheme for machine defect classification. *IEEE Trans Instrumentation and Measurement* 2004; 53(6): 1517–1525.
14. He Q, Yan R, Kong F, et al. Machine condition monitoring using principal component representations. *Mech Sys Signal Process* 2009; 23: 446–466.
15. Egusquiza E, Valero C, Huang X, et al. Failure investigation of a large pump-turbine runner. *Engng Failure Analysis* 2012; 23: 27–34.
16. Arif SJ, Laskar SH and Imdadullah. Measurement of machines vibrations by using a fast rotating magnetic field. In: *International conference on multimedia signal processing and communication technologies* 2011, pp.288–291,17–19 December, IEEE Publication, Aligarh, India.
17. Arif SJ, Imdadullah and Asghar MSJ. Rotating magnetic field based instantaneous angular speed measurement of low speed rotating machines. In: *International conference on multimedia signal processing and communication technologies* 2011, pp.252–255, 17–19 December, IEEE Publication, Aligarh, India.
18. Friswell MI and Adhikari S. Structural health monitoring using shaped sensors. *Mech Sys Signal Process* 2010; 24: 623–635.
19. Chang C and Chen J. Vibration monitoring of motorized spindles using spectral analysis techniques. *Mechatronics* 2009; 19: 726–734.
20. Hestenes MR. Inversion of matrices by biorthogonalization and related results. *J Society Ind Applied Math* 1958; 6(1): 51–90.
21. Henry ER and Hafrichter J. Singular value decomposition: Application to analysis and experimental data. *Essential Numerical Computer Methods* 2010; 210: 81–138.
22. Wall ME, Rechtsteiner A and Rocha LM. Singular value decomposition and principal component analysis. *A practical approach to microarray data analysis*. Springer, 2003, pp.91–109.
23. Cho MS and Kim KJ. Indirect input identification in multi-source environments by principal component analysis. *Mech Sys Signal Process* 2002; 16(5): 873–883.
24. Trendafilova I. An automated procedure for detection and identification of ball bearing damage using multivariate statistics and pattern recognition. *Mech Sys Signal Process* 2010, 1858–1869.
25. Duda RO, Hart PE and Stork DG. *Pattern classification*. 2nd ed. Wiley, 2011.
26. Jolliffe IT. Discarding variables in a principal component analysis. I: artificial data. *J Royal Statistical Society. Series C Applied Statistics* 1972; 21(2): 160–173.
27. Prabhakar S, Sekhar AS and Mohanty AR. Vibration analysis of a misaligned rotar-coupling-bearing system through critical speed. *Proc IMechE, Part C: J Mechanical Engineering Science* 2001; 215(12): 1417–1428.
28. Prabhakar S, Sekhar AS and Mohanty AR. Transient lateral analysis of a slant- cracked rotor passing through its flexural critical speed. *Mechanism and Machine Theory* 2002; 37(9): 1007–1020.